



# High transparent, low surface resistance ZTO/Ag/ZTO multilayer thin film electrodes on glass and polymer substrates

Merve Ekmekcioglu<sup>a</sup>, Nursev Erdogan<sup>b</sup>, Aziz Taner Astarlioglu<sup>b,c</sup>, Serap Yigen<sup>a</sup>, Gulnur Aygun<sup>a</sup>, Lutfi Ozyuzer<sup>a,d</sup>, Mehtap Ozdemir<sup>d,\*</sup>

<sup>a</sup> Department of Physics, Izmir Institute of Technology, Urla, 35430, Izmir, Turkey

<sup>b</sup> Turkish Aerospace, Advanced Material, Process and Energy Technology Center, 06980, Ankara, Turkey

<sup>c</sup> UNAM-National Nanotechnology Research Center and Institute of Materials Science and Nanotechnology, Bilkent University, Ankara, 06800, Turkey

<sup>d</sup> Teknoma Technological Materials Inc., IYTE Campus, Urla, 35430, Izmir, Turkey

## ARTICLE INFO

### Keywords:

Transparent conducting oxides  
Dielectric/metal/dielectric  
ZTO/Ag/ZTO  
Magnetron sputtering

## ABSTRACT

Zinc tin oxide (ZTO)/Ag/ZTO multilayer thin films were grown by direct current (DC) magnetron sputtering technique at room temperature on soda lime glass (SLG) and different polymer substrates such as polycarbonate (PC) and polyethylene terephthalate (PET) for transparent conductive electrode (TCE) applications. The effect of substrate on the structural, optical and electrical characteristics of ZTO/Ag/ZTO multilayers was investigated. All prepared ZTO/Ag/ZTO films presented amorphous structure as expected from room temperature deposition process and smooth surface quality with very low surface roughness. We found that ZTO/Ag/ZTO multilayer films grown on SLG, PET and PC substrates have very high optical transmission and low surface resistance. Moreover, after ZTO/Ag/ZTO multilayer thin film deposition on polymer substrates, the optical transmission was found to be enhanced because the higher absorption due to Ag layer is compensated by lower reflectance. Our results suggest that ZTO/Ag/ZTO multilayer thin films on any substrate can be a promising alternative to indium tin oxide (ITO) films as a cost-effective, indium-free, flexible and transparent electrode for various applications.

## 1. Introduction

The research for transparent conductive electrodes (TCE) is driven by the expanding need for optoelectronic device applications such as solar cells, touch screens, Organic Light Emitting Diodes (OLEDs), Liquid Crystal Displays (LCDs), Light Emitting Diodes (LEDs). There are various transparent conductive oxides (TCOs) such as indium tin oxide (ITO) [1, 2], indium zinc oxide (IZO) [3], gallium zinc oxide (GZO) [4], aluminum zinc oxide (AZO) [5,6], molybdenum-doped indium oxide (IMO) [7] and hydrogenated zinc oxide films (ZnO:H) [8] that have been used in these applications. ITO is the most commonly used TCE in commercial devices due to its high transparency and low sheet resistance. Indium, which is the main constituent of ITO, is known to be an expensive and scarce material [9–11]. Therefore, high pricing and lack of sufficient indium supplies could potentially limit ITO usage in future electronics. In addition, manufacturing high quality ITO thin films requires higher processing temperatures (over 300 °C) which could be a serious hindrance to fabricate ITO films on various substrates. Besides, the increasing demand of ITO as transparent electrode for commercial

products also increase the price of it [12]. Therefore, it is necessary to replace ITO with a better TCE which can be grown at room temperature, and have high transparency and conductivity.

The dielectric/metal/dielectric (DMD) multilayer thin film electrodes have been considered as a promising alternative to ITO film [13]. Single layer TCOs, sputtered at room temperature, have been shown to be highly transparent and conductive, yet these single layer systems can generate a large optical loss (approximately 16%) due to Fresnel reflectance at the interfaces [14]. Recently, functional multilayer thin films consisting of a metal interlayer sandwiched between semiconductor layers have been proposed in order to enhance the electrical and optical properties of TCEs [15]. Some of the recent studies presented detailed design principles for optimizing the performance of the structure [16,17]. Most of these designs consist of two different dielectric layers requiring three target materials. This issue complicates the fabrication process and increases the cost of production. Therefore, for the feasibility of fabrication, simple DMD structures have become more attractive. Especially, Zinc Tin Oxide (ZTO)/Ag/ZTO [18], ITO/Ag/ZTO [19], IZO/Ag/IZO [20], ZTO/Ag/ZTO [21], GZO/Ag/GZO [22],

\* Corresponding author.

E-mail address: [mehtapozdemir@teknoma.net](mailto:mehtapozdemir@teknoma.net) (M. Ozdemir).

<https://doi.org/10.1016/j.vacuum.2021.110100>

Received 6 November 2020; Received in revised form 15 January 2021; Accepted 24 January 2021

Available online 2 February 2021

0042-207X/© 2021 Elsevier Ltd. All rights reserved.

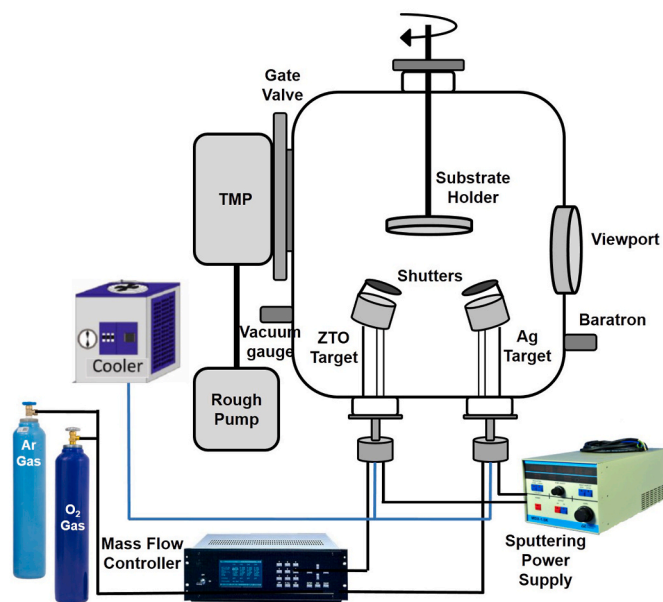


Fig. 1. Schematic diagram of DC magnetron sputtering system.

AZO/Ag/AZO [23], ITO/Ag/ITO [24], ZnO/Ag/ZnO [25] and Niobium Titanium Oxide (NTO)/Ag/NTO [26] have been comprehensively investigated. Among these multilayer thin film electrodes, ZTO/Ag/ZTO is the most preferred one because of its low sheet resistance of about 10  $\Omega$ /sq and high optical transmittance 85.5% at 550 nm in the visible range of the spectrum [18,27].

Another advantage of these DMD multilayer thin film electrodes apart from their feasibility of room temperature fabrication, high optical transmittance and low sheet resistance, they can easily be grown on thermoplastic materials such as polyethylene terephthalate (PET) [28], polycarbonate (PC) [29], polyimide (PI) [30], polyether sulfone (PES) [31] and polyethylene naphthalate (PEN) [32,33]. Thus, they could be applied in flexible electronics. Although there have been some reports demonstrating the room temperature growth of transparent conductive ZTO/Ag/ZTO films on various plastic substrates via sputtering techniques, to the best of our knowledge, ZTO/Ag/ZTO thin films on PC substrate have never been investigated.

In this study, ZTO/Ag/ZTO multilayer thin film electrodes have been grown by DC magnetron sputtering at room temperature on three different substrates; soda lime glass (SLG), PC, and PET to investigate the effect of the substrate. The structural, electrical and optical characterizations of the ZTO/Ag/ZTO multilayer thin film electrodes were performed by using x-ray diffraction (XRD), scanning electron microscopy (SEM), atomic force microscopy (AFM), Raman spectroscopy and UV/Vis/NIR spectrophotometry techniques.

## 2. Experimental

ZTO/Ag/ZTO multilayer thin films were grown by DC magnetron sputtering technique without any substrate heating process under high vacuum on 1.0 mm thick SLG, 21 mm thick PC and 75  $\mu$ m thick PET. It is mentioned in many publications that RF and DC magnetron sputtering are the best techniques for fabrication of ZTO [12]. The sputtering was done using a ZTO target (2 in.) with a Zn:Sn atomic ratio of 2:1 which is thermodynamically stable. The substrates were cleaned in an ultrasonic bath in alcohol and de-ionized water sequentially for 10 min. The cleaning process was followed by an oxygen plasma treatment for 10 min to eliminate organic residue from the surface. Then the samples were placed into the vacuum chamber as shown in Fig. 1. The vacuum chamber was first evacuated to a pressure of  $< 5 \times 10^{-2}$  Torr by a rough pump, then a base pressure of less than  $2 \times 10^{-6}$  Torr was achieved

Table 1

Sheet resistance and transmission data for ZTO/Ag/ZTO/SLG multilayer thin films having different Ag deposition rate.

Sample	Ag Deposition Time(s)	Sheet Resistance ( $\Omega$ /sq)	Transmission at 550 nm (%)
SLG	-	-	91.6
ZTO/Ag/ZTO-1	20	$11.7 \pm 0.2$	90.4
ZTO/Ag/ZTO-2	21	$10.4 \pm 0.2$	89.6
ZTO/Ag/ZTO-3	22	$9.9 \pm 0.2$	91.2
ZTO/Ag/ZTO-4	23	$8.1 \pm 0.2$	89.0

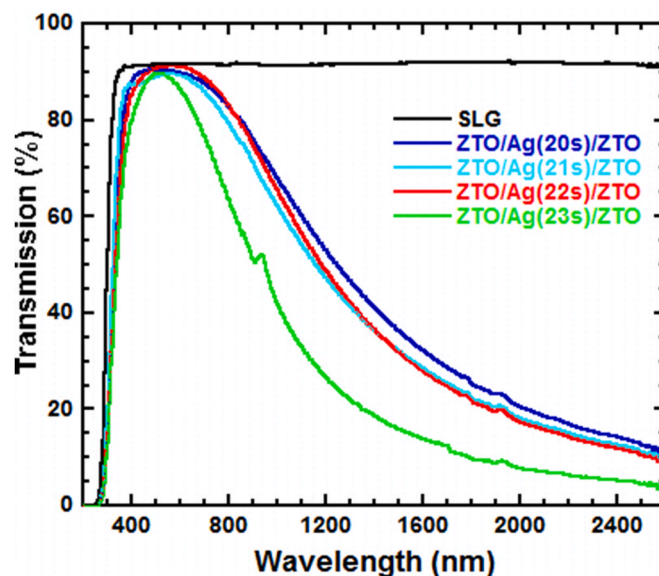


Fig. 2. Optical transmittance spectra of ZTO/Ag/ZTO/SLG with various Ag deposition time.

using a turbo molecular pump (TMP) under Ar gas flow. The working gas pressure, target to substrate distance and the sputtering power were set as  $2.0 \times 10^{-3}$  Torr, 7.5 cm and 15 W, respectively. Prior to each deposition process, the surfaces of ZTO and Ag targets were pre-sputtered in the Ar environment for 10 min in order to remove the native oxide layer.

The deposition process started with sputtering first ZTO layer for 10 min, then Ag interlayer was sputtered and finally, ZTO layer was sputtered for 10 min on top. The deposition time for Ag layer was varied from 20 to 23 s and Transmission (%) and Sheet Resistance of ZTO/Ag/ZTO structures were measured. Table 1 presents the obtained results with respect to Ag deposition time and Fig. 2 shows the optical transmittance spectra acquired from blank SLG and ZTO/Ag/ZTO/SLG samples. Based on these results, 22 s was found to be the optimum deposition time for Ag layer which gives the highest transmittance and

Table 2

The optimized growth conditions for ZTO/Ag/ZTO multilayer thin films.

Deposition Parameters	Sputtering Conditions
Base pressure (Torr)	$< 2 \times 10^{-6}$ Torr
Deposition pressure (Torr)	$2 \times 10^{-3}$ Torr
DC power (W)	ZTO: 15 W, Ag: 15 W
Target-substrate distance (cm)	7.5 cm
Ar gas flow rate (sccm)	ZTO: 30 sccm, Ag: 40 sccm
Deposition Time	ZTO: 10 min, Ag: 22s
Substrate temperature	Room temperature

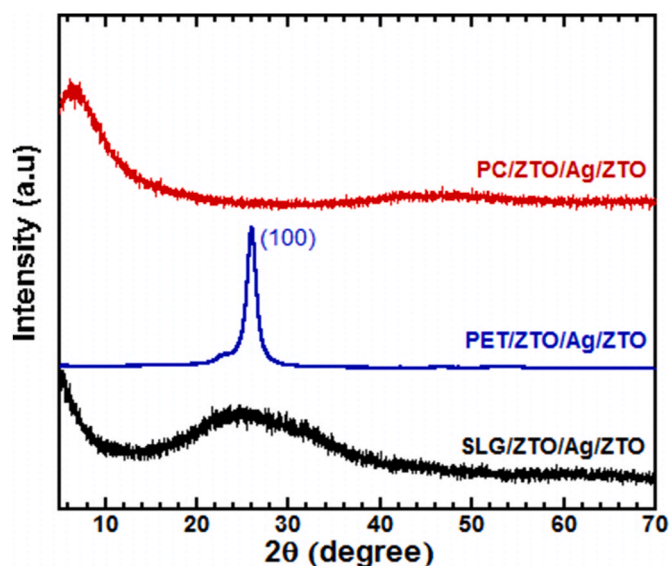


Fig. 3. XRD spectra of ZTO/Ag/ZTO films on SLG, PET and PC substrates.

low sheet resistance. Because, when the deposition time was less than 22 s, Ag adatoms are homogeneously distributed on ZTO layer, however they do not electrically connect to each other to form a continuous film. In addition, the grain size in the Ag layer was increased which led to a decrease in grain-boundary scattering [34]. Therefore, the effect of Ag layer was not observed in the optical and electrical properties of the ZTO/Ag/ZTO multilayer as seen in Table 1.

Above a hundred sample were deposited for this study. After optimum parameters given in Table 2 were obtained, ZTO/Ag/ZTO multilayer films were grown on three type of substrates. All the deposition processes were performed at room temperature to prevent heating of the polymer substrates. On the other hand, the temperature of the substrate was measured to be reaching about 60–70 °C during sputtering process.

The thicknesses of the ZTO/Ag/ZTO samples were measured by a surface profilometer (Veeco DEKTAK 150). The structural characterizations were comprehensively studied via XRD measurements performed with Phillips X' Pert Pro X-ray diffractometer using Cu K $\alpha$  radiation ( $\lambda = 1.5406 \text{ \AA}$ ) at a scanning rate of 0.016°/s in the 2 $\theta$  range of 20°–70°. The surface morphology was investigated with SEM images (FEI-Quanta FEG 250 SEM) captured at an operating voltage of 20 kV. The surface topography and root mean square (RMS) roughness were analyzed by AFM scans of 5  $\mu\text{m} \times 5 \mu\text{m}$ . Raman measurements were performed by micro-Raman spectrometer (S&I Mono Vista Raman System, 0.750 mm Imaging Triple Grating Monochromator) using Ar-ion laser with excitation wavelength of 514.5 nm at 25 mW for both ZTO and ZTO/Ag/ZTO samples. Calibration was done using Si main mode at 521  $\text{cm}^{-1}$  and the measurements were taken with 600 gratings using 100x objective. The surface resistances of ZTO/Ag/ZTO electrodes were obtained by a four-point probe system equipped with a Keithley 2425 instrument. The transmittance data were acquired by PerkinElmer Lambda 950 UV/Vis/NIR spectrophotometer between 200 and 2600

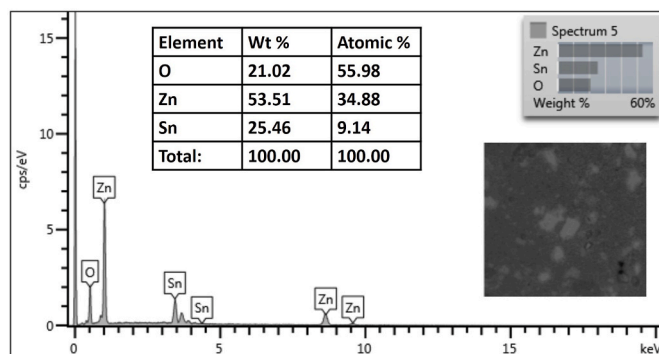


Fig. 5. EDX analysis of ZTO Target.

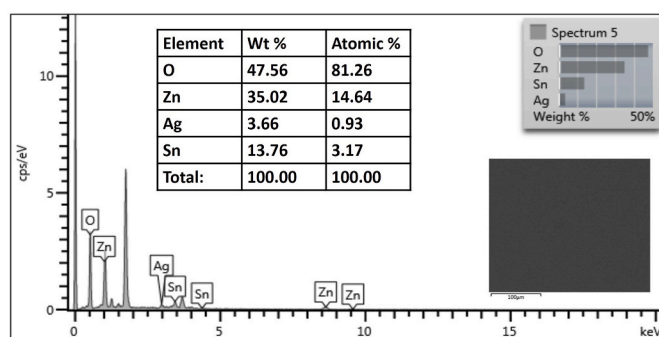


Fig. 6. EDX analysis of ZTO/Ag/ZTO/SLG multilayer thin film electrodes.

nm.

### 3. Results and discussion

The thickness of each layer in ZTO/Ag/ZTO multilayer was obtained from thickness profile as 40 nm for ZTO and 9.5 nm for Ag layers. In addition, the total thickness of the multilayer structure on glass, PET and PC substrate was measured as 90 nm.

Comparison of XRD patterns of ZTO/Ag/ZTO films deposited on SLG, PET and PC substrates is given in Fig. 3. No crystalline peaks were observed in any XRD spectra except for the one at 25.9° which is the main diffraction peak of the PET substrate, as PET is a typical semi-crystalline thermoplastic [35]. Consistent with the literature [18], XRD analysis confirmed that all ZTO/Ag/ZTO films grown at room temperature were found in amorphous state. Thanks to its amorphous structure and the comparatively high flexibility of choosing deposition parameters, ZTO/Ag/ZTO is well suited for TCE applications.

The surface morphology was extensively investigated by SEM analysis. Fig. 4 presents the SEM images of ZTO/Ag/ZTO multilayer structures deposited on SLG, PC and PET substrates. All ZTO/Ag/ZTO multilayer thin film electrodes on the three different substrates exhibited very smooth and flat surface without any defects like cracks pinholes, pores and protrusion. The roughness seen on the ZTO/Ag/ZTO

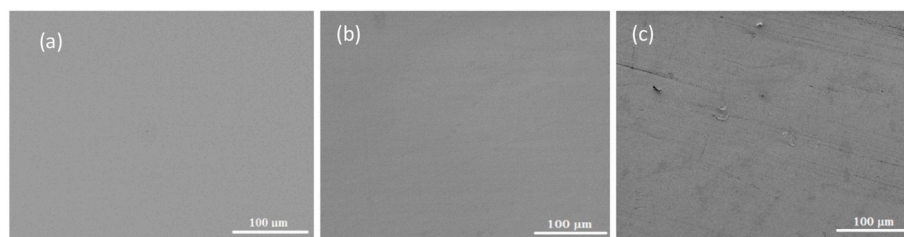
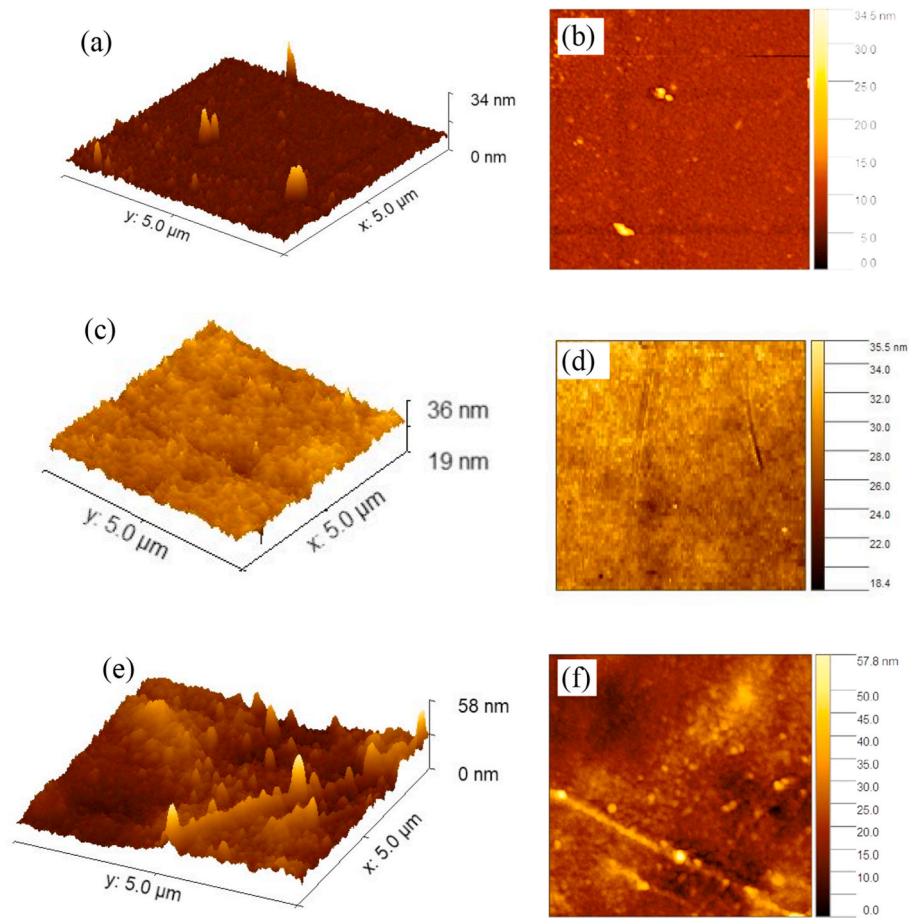


Fig. 4. SEM images of (a) ZTO/Ag/ZTO/SLG, (b) ZTO/Ag/ZTO/PC and ZTO/Ag/ZTO/PET multilayer thin film electrodes.





**Fig. 7.** (a) 3D and (b) 2D AFM images of ZTO/Ag/ZTO/SLG, (c) 3D and (d) 2D AFM images of ZTO/Ag/ZTO/PC, (e) 3D and (f) 2D AFM images of ZTO/Ag/ZTO/PET samples.

thin film grown on PET substrate was caused by the surface of the substrate underneath. The smoothness of TCE surface is extremely significant for the applications, because such structural imperfections can cause serious break down or short-circuit problems in various electronic devices.

The atomic concentrations of ZTO target used for sputtering (Fig. 5) and as deposited ZTO/Ag/ZTO thin films on SLG (Fig. 6) were determined by EDX analyses. EDX results showed that while the Zn/Sn ratio was 3.8 for ZTO target, it was 4.6 for ZTO/Ag/ZTO film on SLG. This difference in Zn/Sn ratios results from some of the tin evaporating away from the structure during the coating process. When the surface of the ZTO target is examined, white areas are seen on the surface. This is due to the presence of different stoichiometry rates on the surface of the target. EDX analysis of target were taken after racetrack was formed on surface of 2-inch target by deposition process. The phase segregation was occurred and the atomic concentration was changed by Ar ion bombardment. On the other hand, there was no texture on the film surface grown by using this target.

The surface topographies of the ZTO/Ag/ZTO multilayer thin films deposited on SLG, PC and PET substrates were investigated by two (2D) and three-dimensional (3D) AFM images shown in Fig. 7. The RMS roughnesses of these electrodes at room temperature were calculated as 1.45 nm for SLG, 3.00 nm for PC and 5.90 nm for PET substrates. The low surface roughness is one of the most important advantage of the ZTO/Ag/ZTO multilayer thin films to be used as TCEs in optoelectronic device applications, because smooth surface can prevent possible shunts and leakage current in the devices [25,26].

Raman spectroscopy analysis was performed to investigate the structural properties of ZTO/SLG and ZTO/Ag/ZTO/SLG samples.

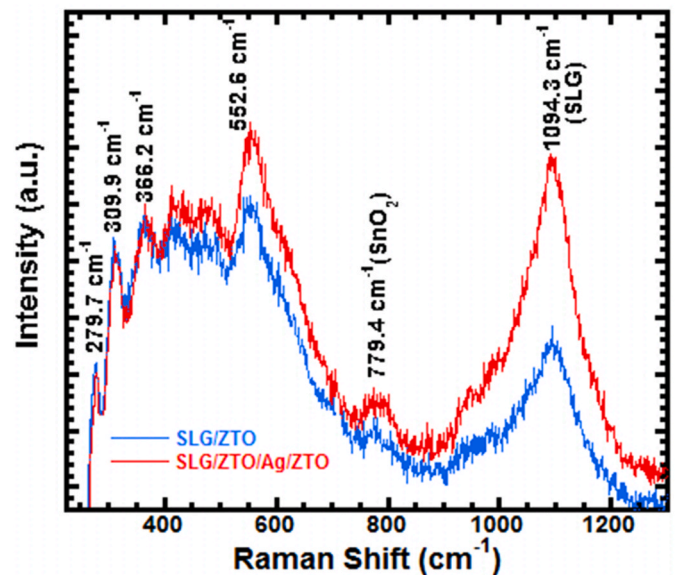


**Fig. 8.** Raman spectra of ZTO/SLG and ZTO/Ag/ZTO/SLG thin films.

Raman spectrum of ZTO/SLG thin film at room temperature is depicted in Fig. 8. Raman peaks appearing at  $309.9\text{ cm}^{-1}$  and  $366.2\text{ cm}^{-1}$  can be attributed to E (LO) and A<sub>1</sub> (LO) symmetries, respectively, in ZnSnO<sub>3</sub> whereas the peak at  $776.4\text{ cm}^{-1}$  is assigned to the B<sub>2g</sub> (asymmetric Sn–O

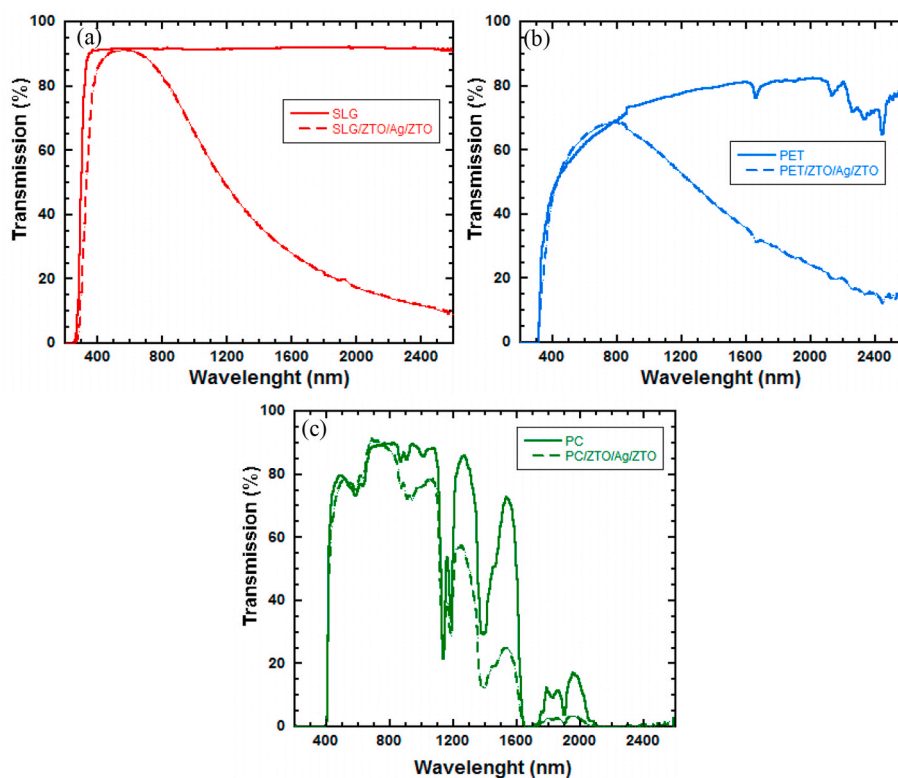


Fig. 9. Optical transmittance spectra for uncoated and ZTO/Ag/ZTO-coated (a) SLG, (b) PET and (c) PC substrates.

Table 3

Sheet resistance and optical transmittance of ZTO/Ag/ZTO multilayer thin films deposited on SLG, PC and PET substrates.

Samples	Sheet Resistance (ohm/sq)	Transmittance at 550 nm (%)
SLG	–	91.6
ZTO/Ag/ZTO/SLG	$8.6 \pm 0.2$	91.2
PC	–	75.7
ZTO/Ag/ZTO/PC	$6.7 \pm 0.2$	77.2
PET	–	59.2
ZTO/Ag/ZTO/PET	$11.2 \pm 0.2$	62.0

stretching) vibration modes of  $\text{SnO}_2$  [36]. A broad Raman peak at  $1094.3 \text{ cm}^{-1}$  is related to the SLG substrate [37]. According to the literature [36],  $\text{ZnSnO}_3$  peaks are observed in Raman spectra of the samples grown at room temperature. With a heat treatment up to  $500^\circ\text{C}$ ,  $\text{Zn}_2\text{SnO}_4$  phases appear at  $521 \text{ cm}^{-1}$  and  $669 \text{ cm}^{-1}$  [38–40]. However, due to the room temperature processing, these peaks were not observed in the present study.

The optical transmittance data as a function of wavelength for uncoated and ZTO/Ag/ZTO coated substrates are given in Fig. 9. The optical transmittance values at 550 nm were found to be 91.6% for SLG (Figs. 9a), 59.2% for PET (Figs. 9b) and 77.2% for PC (Fig. 9c) substrates. The optical transmittance and sheet resistance measurements are summarized in Table 3 for ZTO(10min)/Ag(22s)/ZTO(10min) layers deposited onto SLG, PET and PC substrates. The results clearly indicate that all ZTO/Ag/ZTO multilayer thin films are highly transparent at 550 nm which is a remarkable achievement when compared to other popular TCOs used in commercial products. For example, transmission of the most preferred transparent electrode, ITO, is about 85% on SLG [1,41] and 75% on PC [42]. Besides, we found that ZTO/Ag/ZTO films deposited on PC and PET substrates show enhanced optical transmission. Minimum reflection is obtained because of the absorption taking place in the silver thin film layer [16]. To explain this phenomenon; absorption, transmission and reflection of ZTO/Ag/ZTO

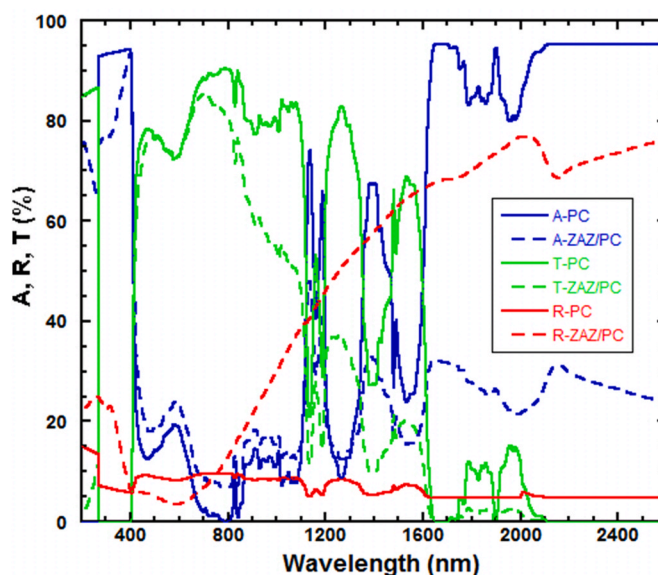


Fig. 10. Simulated absorption, transmission and reflection data of ZTO/Ag/ZTO/PC sample.

multilayer on PC substrate was simulated using OpenFilters Software [43]. Fig. 10 shows the simulation results of transmission, absorption and reflection of the uncoated and ZTO/Ag/ZTO coated PC substrates over the wavelength range 200–2600 nm. As seen in the figure, the simulated transmission data are well matched for uncoated and coated substrates indicating the enhanced transmission of substrates at 550 nm. In addition, it was found that the absorption values of the coated substrates increase while their reflection decreases at 550 nm. This indicates that, the absorption takes place in the silver thin film layer so reflection

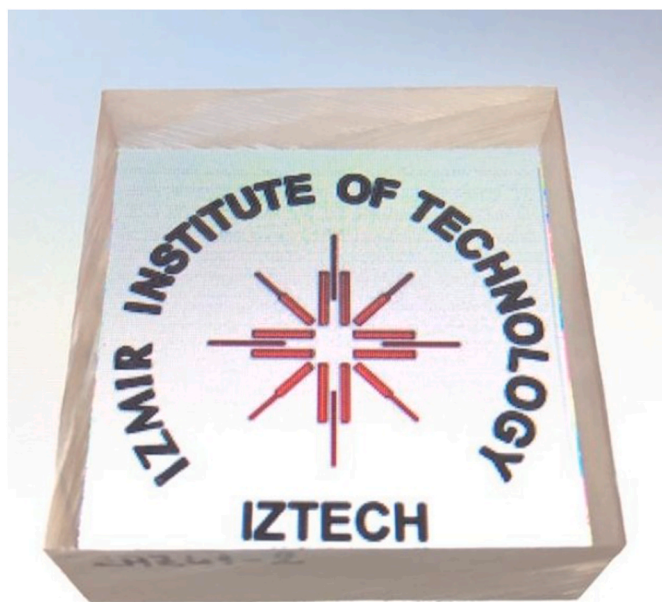


Fig. 11. Photograph of a ZTO/Ag/ZTO/PC sample over IZTECH logo.

decreases and transmission enhances.

A photographic image of the ZTO/Ag/ZTO multilayer thin film coated on a 21 mm thick PC substrate is shown in Fig. 11. As seen in the picture, the logo can be clearly seen through the coated PC substrate since the ZTO/Ag/ZTO multilayer film coating is highly transparent.

#### 4. Conclusions

In this study, ZTO/Ag/ZTO multilayer thin film electrodes were fabricated by DC magnetron sputtering onto various transparent substrates, such as SLG, PC and PET. The structural, optical and electrical properties of deposited ZTO/Ag/ZTO electrodes were extensively studied. As a result of the present investigation, it was shown that ZTO/Ag/ZTO multilayer films are highly transparent and conductive compared to conventional TCOs. Especially, high optical transmittance (77%) and low sheet resistance ( $6.7 \Omega/\text{square}$ ) of ZTO/Ag/ZTO multilayer film deposited on 21 mm thick PC substrate at room temperature could be useful for various device applications, since ZTO/Ag/ZTO multilayer thin film deposited on PC and PET substrates showed an enhanced transmission due to the higher absorption and lower reflection occurred in Ag thin film layer and a decrease in grain-boundary scattering. While the transmission of uncoated PC and PET are 75.9% and 58%, coated PC and PET are found to be 77% and 62% at 550 nm, respectively. In addition, ZTO/Ag/ZTO multilayer thin film electrodes on all substrates exhibited very smooth surface with very low roughness, which is essential for developing high performance OLEDs. This surface quality could also be very advantageous for optoelectronic device applications, as it can prevent break down or short-circuit. In addition, low surface roughness of the ZTO/Ag/ZTO multilayer thin film electrodes could help suppressing possible shunts and leakage current in the devices. As a result, because of their excellent electrical and optical properties, ZTO/Ag/ZTO electrodes can be a promising candidate for TCE applications. The present work provides a good platform to further study room temperature fabrication of flexible TCEs and thus develop novel flexible optoelectronic devices.

#### Declaration of competing interest

The authors declare that they have no known competing financial interests or personal relationships that could have appeared to influence the work reported in this paper.

#### Acknowledgments

This work was supported by Turkish Aerospace Industries with the project number of TM0131 and TUBITAK (Scientific and Technical Research Council of Turkey) project numbers 1170129 and 5189901. The authors would like to acknowledge the facilities of Research and Application Center for Quantum Technologies (RACQUT) for the current study.

#### References

- [1] O. Tuna, Y. Selamet, G. Aygun, L. Ozyuzer, High quality ITO thin films grown by dc and RF sputtering without oxygen, *J. Phys. D Appl. Phys.* 43 (2010), <https://doi.org/10.1088/0022-3727/43/5/055402>.
- [2] H. Koseoglu, F. Turkoglu, M. Kurt, M.D. Yaman, G.K. Akca, G. Aygun, L. Ozyuzer, Improvement of optical and electrical properties of ITO thin films by electro-annealing, *Vacuum* 120 (2015) 8–13, <https://doi.org/10.1016/j.vacuum.2015.06.027>.
- [3] J.J. Lee, J.S. Kim, S.J. Yoon, Y.S. Cho, J.W. Choi, Electrical and optical properties of indium zinc oxide (IZO) thin films by continuous composition spread, *J. Nanosci. Nanotechnol.* 13 (2013) 3317–3320, <https://doi.org/10.1166/jnn.2013.7274>.
- [4] E. Muchuweni, T.S. Sathiaraj, H. Nyakoty, Effect of gallium doping on the structural, optical and electrical properties of zinc oxide thin films prepared by spray pyrolysis, *Ceram. Int.* 42 (2016) 10066–11007, <https://doi.org/10.1016/j.ceramint.2016.03.110>.
- [5] A. Eshaghi, M. Hajkarimi, Optical and electrical properties of aluminum zinc oxide (AZO) nanostructured thin film deposited on polycarbonate substrate, *Optik* 125 (2014) 5746–5749, <https://doi.org/10.1016/j.ijleo.2014.07.056>.
- [6] F. Turkoglu, H. Koseoglu, S. Zeybek, M. Ozdemir, G. Aygun, L. Ozyuzer, Effect of substrate rotation speed and off-center deposition on the structural, optical, and electrical properties of AZO thin films fabricated by DC magnetron sputtering, *J. Appl. Phys.* 123 (2018) 165104, <https://doi.org/10.1063/1.5012883>.
- [7] S. Parthiban, V. Gokulakrishnan, K. Ramamurthi, E. Elangovan, R. Martins, E. Fortunato, R. Ganesan, High near-infrared transparent molybdenum-doped indium oxide thin films for nanocrystalline silicon solar cell applications, *Sol. Energy Mater. Sol. Cells* 93 (2009) 92–97, <https://doi.org/10.1016/j.solmat.2008.08.007>.
- [8] D. Gaspar, L. Pereira, K. Gehrke, B. Galler, E. Fortunato, R. Martins, High mobility hydrogenated zinc oxide thin films, *Sol. Energy Mater. Sol. Cells* 163 (2017) 255–262, <https://doi.org/10.1016/j.solmat.2017.01.030>.
- [9] T. Minami, Transparent conducting oxide semiconductors for transparent electrodes, *Semicond. Sci. Technol.* 20 (2005), <https://doi.org/10.1088/0268-1242/20/4/004>.
- [10] L. Castañeda, Present status of the development and application of transparent conductors oxide thin solid films, *Mater. Sci. Appl.* 2 (2011) 1233–1242, <https://doi.org/10.4236/msa.2011.29167>.
- [11] S. Edinger, N. Bansal, M. Bauch, R.A. Wibowo, G. Újvári, R. Hamid, G. Trimmel, T. Dimopoulos, Highly transparent and conductive indium-doped zinc oxide films deposited at low substrate temperature by spray pyrolysis from water-based solutions, *J. Mater. Sci.* 52 (2017) 8591–8602, <https://doi.org/10.1007/s10853-017-1084-8>.
- [12] M. Coll, J. Fontcuberta, M. Althammer, et al., Towards oxide electronics: a roadmap, *Appl. Surf. Sci.* 482 (2019) 1–93, <https://doi.org/10.1016/j.apsusc.2019.03.312>.
- [13] K. Ellmer, Past achievements and future challenges in the development of optically transparent electrodes, *Nat. Photon.* (2012), <https://doi.org/10.1038/nphoton.2012.282>.
- [14] C.H. Hong, J.H. Shin, B.K. Ju, K.H. Kim, N.M. Park, B.S. Kim, W.S. Cheong, Index-matched indium tin oxide electrodes for capacitive touch screen panel applications, *J. Nanosci. Nanotechnol.* 13 (2013) 7756–7759, <https://doi.org/10.1166/jnn.2013.7814>.
- [15] S. Ozbay, N. Erdogan, F. Erden, M. Ekmekcioglu, M. Ozdemir, G. Aygun, L. Ozyuzer, Surface free energy analysis of ITO/Au/ITO multilayer thin films on polycarbonate substrate by apparent contact angle measurements, *Appl. Surf. Sci.* 529 (2020) 147111, <https://doi.org/10.1016/j.apsusc.2020.147111>.
- [16] R.A. Maniyara, V.K. Mkhitarian, T.L. Chen, D.S. Ghosh, V. Pruneri, An antireflection transparent conductor with ultralow optical loss (<2 %) and electrical resistance (< $6\Omega\text{sq}^{-1}$ ), *Nat. Commun.* (2016), <https://doi.org/10.1038/ncomms13771>.
- [17] C. Ji, D. Liu, C. Zhang, L. Jay Guo, Ultrathin-metal-film-based transparent electrodes with relative transmittance surpassing 100%, *Nat. Commun.* 11 (2020) 1–8, <https://doi.org/10.1038/s41467-020-17107-6>.
- [18] S.H. Cho, R. Pandey, C.H. Wie, Y.J. Lee, J.W. Lim, D.H. Park, J.S. Seok, Y.H. Jang, K.K. Kim, D.K. Hwang, D.J. Byun, W.K. Choi, Highly transparent ZTO/Ag/ZTO multilayer electrode deposited by inline sputtering process for organic photovoltaic cells, *Phys. Status Solidi Appl. Mater. Sci.* 211 (2014) 1860–1867, <https://doi.org/10.1002/pssa.201330594>.
- [19] S.M. Lee, H.W. Koo, T.W. Kim, H.K. Kim, Asymmetric ITO/Ag/ZTO and ZTO/Ag/ITO anodes prepared by roll-to-roll sputtering for flexible organic light-emitting diodes, *Surf. Coatings Technol.* 343 (2018) 115–120, <https://doi.org/10.1016/j.surfcoat.2017.10.048>.
- [20] S.H. Choa, C.K. Cho, W.J. Hwang, K. Tae Eun, H.K. Kim, Mechanical integrity of flexible InZnO/Ag/InZnO multilayer electrodes grown by continuous roll-to-roll



- sputtering, *Sol. Energy Mater. Sol. Cells* 95 (2011) 3442–3449, <https://doi.org/10.1016/j.solmat.2011.08.001>.
- [21] S. Hong, S.H. Kang, Y. Kim, C.W. Jung, Transparent and flexible antenna for wearable glasses applications, *IEEE Trans. Antenn. Propag.* 64 (2016) 2797–2804, <https://doi.org/10.1109/TAP.2016.2554626>.
- [22] Y.S. Park, H.K. Kim, S.W. Kim, Thin Ag layer inserted GZO multilayer grown by roll-to-roll sputtering for flexible and transparent conducting electrodes, *J. Electrochem. Soc.* 157 (2010) 301–306, <https://doi.org/10.1149/1.3454125>.
- [23] G. Torrisi, I. Crupi, S. Mirabella, A. Terrasi, Robustness and electrical reliability of AZO/Ag/AZO thin film after bending stress, *Sol. Energy Mater. Sol. Cells* 165 (2017) 88–93, <https://doi.org/10.1016/j.solmat.2017.02.037>.
- [24] K. Choi, J. Kim, Y. Lee, H. Kim, ITO/Ag/TTO multilayer films for the application of a very low resistance transparent electrode, *Thin Solid Films* 341 (1999) 152–155, [https://doi.org/10.1016/S0040-6090\(98\)01556-9](https://doi.org/10.1016/S0040-6090(98)01556-9).
- [25] J. Ho Kim, J. Hwan Lee, S.-W. Kim, Y.-Z. Yoo, T.-Y. Seong, Highly flexible ZnO/Ag/ZnO conducting electrode for organic photonic devices, *Ceram. Int.* 41 (2015) 7146–7150, <https://doi.org/10.1016/j.ceramint.2015.02.031>.
- [26] J.H. Park, H.K. Kim, H. Lee, H. Lee, S. Yoon, C.D. Kim, Highly transparent, low resistance, and cost-efficient Nb: TiO<sub>2</sub>/Ag/Nb: TiO<sub>2</sub> multilayer electrode prepared at room temperature using black Nb: TiO<sub>2</sub> target, *Electrochem. Solid State Lett.* 13 (2010), <https://doi.org/10.1149/1.3313361>.
- [27] H. Schmidt, T. Winkler, T. Riedl, I. Baumann, H. Flügge, S. Schmale, H. Johannes, T. Rabe, S. Hamwi, W. Kowalsky, Highly transparent and conductive ZTO/Ag/ZTO multilayer top electrodes for large area organic solar cells, *Energy Procedia* 31 (2011) 110–116, <https://doi.org/10.1016/j.egypro.2012.11.172>.
- [28] C.J. Chiang, C. Winscom, S. Bull, A. Monkman, Mechanical modeling of flexible OLED devices, *Org. Electron.* 10 (2009) 1268–1274, <https://doi.org/10.1016/j.orgel.2009.07.003>.
- [29] S. Il Kim, K.W. Lee, B.B. Sahu, J.G. Han, Flexible OLED fabrication with ITO thin film on polymer substrate, *Jpn. J. Appl. Phys.* 54 (2015), 090301, <https://doi.org/10.7567/JJAP.54.090301>.
- [30] K.M. Lee, R. Fardel, L. Zhao, C.B. Arnold, B.P. Rand, Enhanced outcoupling in flexible organic light-emitting diodes on scattering polyimide substrates, *Org. Electron.* 51 (2017) 471–476, <https://doi.org/10.1016/j.orgel.2017.09.042>.
- [31] P.H. Lei, C.M. Hsu, Y.S. Fan, Flexible organic light-emitting diodes on a polyestersulfone (PES) substrate using Al-doped ZnO anode grown by dual-plasma-enhanced metalorganic deposition system, *Org. Electron.* 14 (2013) 236–249, <https://doi.org/10.1016/j.orgel.2012.10.030>.
- [32] E. Fortunato, A. Goncalves, A. Marques, A. Viana, H. Aguas, L. Pereira, I. Ferreira, P. Vilarinho, R. Martins, New developments in gallium doped zinc oxide deposited on polymeric substrates by RF magnetron sputtering, *Surf. Coating Technol.* 180 (2004) 20–25, <https://doi.org/10.1016/j.surfcoat.2003.10.025>.
- [33] M.G. Sandoval-Paz, R. Ramírez-Bon, Indium tin oxide films deposited on polyethylene naphthalate substrates by radio frequency magnetron sputtering, *Thin Solid Films* 517 (2009) 2596–2601, <https://doi.org/10.1016/j.tsf.2008.10.016>.
- [34] J. Kim, S. Kim, S. Yoon, P. Song, Characteristics of ITO/Ag/ITO hybrid layers prepared by magnetron sputtering for transparent film heaters, *J. Opt. Soc. Korea* 20 (2016) 807–812, <https://doi.org/10.3807/JOSK.2016.20.6.807>.
- [35] C. Guillén, J. Herrero, Structural, optical and electrical characteristics of ITO thin films deposited by sputtering on different polyester substrates, *Mater. Chem. Phys.* 112 (2008) 641–644, <https://doi.org/10.1016/j.matchemphys.2008.06.027>.
- [36] T. Bora, M.H. Al-Hinai, A.T. Al-Hinai, J. Dutta, Phase transformation of metastable ZnSnO<sub>3</sub> upon thermal decomposition by in-situ temperature-dependent Raman spectroscopy, *J. Am. Ceram. Soc.* 98 (2015) 4044–4049, <https://doi.org/10.1111/jace.13791>.
- [37] I. Saafi, R. Dridi, R. Mimouni, A. Amlouk, A. Yumak, K. Boubaker, P. Petkova, M. Amlouk, Microstructural and optical properties of SnO<sub>2</sub>-ZnSnO<sub>3</sub> ceramics, *Ceram. Int.* 42 (2016) 6273–6281, <https://doi.org/10.1016/j.ceramint.2016.01.010>.
- [38] J. Zeng, M. Di Xin, K.W. Li, H. Wang, H. Yan, W. Zhang, Transformation process and photocatalytic activities of hydrothermally synthesized Zn<sub>2</sub>SnO<sub>4</sub> nanocrystals, *J. Phys. Chem. C* 112 (2008) 4159–4167, <https://doi.org/10.1021/jp7113797>.
- [39] J.X. Wang, S.S. Xie, H.J. Yuan, X.Q. Yan, D.F. Liu, Y. Gao, Z.P. Zhou, L. Song, L. F. Liu, X.W. Zhao, X.Y. Dou, W.Y. Zhou, G. Wang, Synthesis, structure, and photoluminescence of Zn<sub>2</sub>SnO<sub>4</sub> single-crystal nanobelts and nanorings, *Solid State Commun.* 131 (2004) 435–440, <https://doi.org/10.1016/j.ssc.2004.06.009>.
- [40] L. Wang, X. Zhang, X. Liao, W. Yang, A simple method to synthesize single-crystalline Zn<sub>2</sub>SnO<sub>4</sub> (ZTO) nanowires and their photoluminescence properties, *Nanotechnology* 6 (2005), <https://doi.org/10.1088/0957-4484/16/12/034>, 2928–293.
- [41] D. Kudryashov, A. Gudovskikh, K. Zelentsov, Low temperature growth of ITO transparent conductive oxide layers in oxygen-free environment by RF magnetron sputtering, *J. Phys. Conf.* 461 (2013), 012021, <https://doi.org/10.1088/1742-6596/461/1/012021>.
- [42] L. Jing, G. Jian, G. Zhen'an, Preparation of indium tin oxide films on polycarbonate substrates by radio-frequency magnetron sputtering, *J. Wuhan Univ. Technol.-Materials Sci. Ed.* 20 (2005) 22–25.
- [43] S. Larouche, L. Martinu, OpenFilters: open-source software for the design, optimization, and synthesis of optical filters, *Appl. Optic.* 47 (2008) 219–230.